Global Tuning of Local Molecular Phenomena: An Alternative Approach to Bionanoelectronics

Anirban Bandyopadhyay,*,† K. Nittoh,‡ Y. Wakayama,§ S. Yagi,‡ and K. Miki‡

International Center for Young Scientists, National Institute of Material Science, 1−1 Namiki, Tsukuba, Ibaraki 305-0044, Japan, Nanoarchitecture Group, National Institute of Material Science, 1-1 Namiki, Tsukuba, Ibaraki 305-0044, Japan, and Nanoassembly Group, National Institute of Materials Science, 1−1 Namiki, Tsukuba, Ibaraki 305-0044, Japan

Received: April 14, 2006; In Final Form: June 21, 2006

We have applied simultaneous horizontal and vertical bias to a single molecule (2 nm^2) in an ordered and disordered matrix to virtually isolate and tune its property without taking it out physically from its environment. Using a dedicated electrode system, we have locally tuned nanoscale properties vertically by STM, while stabilizing its environment by applying a global electric field horizontally. Using this technique, we report tuning of molecular conformations in room temperature, whose evolution of states has been statistically investigated. We have also shown control on switching of a few selected conformations by applying dual bias simultaneously. As we avoid any direct injection of charge into the system via electrode contact, this technique could be used as a generalized method to tune phenomena evolved in an environment of weak interaction from a large distance without destroying the property.

Intoduction

Utopia created by nanoscale electronics and mechanics is now at a critical phase of existence because of its unstable performance at nanoscale[1] (∼1−6 nm), while footsteps of conventional silicon devices are getting closer and closer[2] (∼20 nm). To understand a pristine system, e.g., a molecule for electronic bionanosystems like DNA for genetics, computations, and nanoelectromechanical systems (NEMS) for nanomachines, we need to isolate and fix each unit between two atomic electrodes with proper orientation.[3] This is ideally a matter of chance,[4] and reliable transmission of generated information to the output depends on orbital coupling and self-energy of the system and channel together.[5] If each unit is self-assembled on an atomic flat surface and specifically pointed by an atomic sharp symmetric STM tip on a typical part of its body, then very local control (2−3 nm^2) might be developed.[6] Yet the environment of nanoscale systems is extremely sensitive due to weak interactions (like strong dipole−dipole interaction) between system units, thermal diffusion, polarization, H bonding, etc.[7] These interactions spontaneously perturb the conformation of a basic system that is coupled with an STM tip and substrate by a local field, generating compound properties rather than individual ones. When a population of molecules undergoes a series of events, "single molecule spectroscopy"[8] and several methods[9] offer either ensemble or completely independent vision,[10] while our objective is midway between two extreme cases: in a phenomenon, evolution of the phase of each molecule during the course of events should not get lost even if it is in the interconnected cluster.

Collective response is enhanced in random distribution of such nanoscale units, and asymmetry in its structure adds to its environment-dependent output. Most of the bionanoelectronic and mechanical systems in nature evolve at nanoscale in fuzzy-assembly and chaotically transmitted generating global properties.[11] Hence, if we could isolate each system unit without taking it out physically from its cluster, we could channelize and traffic the interaction, signal transmission, and chemical reaction evolving at that particular point towards a particular direction of our choice.[12] Long-lasting debates on the true mechanism of such phenomena may come to light.[13]

This present work is driven by the philosophy that if we could apply dual mode control to a system, i.e., locally tuning the system properties with an atomic probe while stabilizing its surrounding environment by a global field, then we might virtually isolate a single nanoscale system without taking it out from its assembly. We have optimized such a dedicated electrode architecture and successfully tuned the bandwidth of a conformational transition spectrum of a typical dye, whose structure is drawn to twist permanently ($\tau \sim 10$ ms, in liquid), into typical conformations known as "dark state".[14] An array of voltage pulses of different height is sent to a "substrate−molecule−tip" unit under UHV-STM (10^{-8} Torr). We observe the transition of its unique molecular geometries between any two pulses and identify a theoretically predicted conformation energy spectrum. A single xanthene dye in a quantum well shows Gaussian probabilistic distribution of transition to different conformations. The bandwidth of the Q-band of Gaussian distribution was tuned by horizontal bias to a maximum of 25%, which revealed that we could successfully control the nanoscale environment of a dye[15] without taking it out physically from its assembly.

Experimental Section

To isolate and fix the nanoscale systems, our approach is novel in two ways. First, we strongly couple the processing surface P1 (Figure 1a−c) with a three external electrode B1, B2, and B3 (voltage varied in pairs B1−B2, B1−B3, B2−B3,

* Corresponding author. E-mail: anirban.bandyo@rediffmail.com. Telephone: 0081-29-851-3354 Ext. 8918 or 8840. Fax: 0081-29-860-4706.
† International Center for Young Scientists.
‡ Nanoarchitecture Group.
§ Nanoassembly Group.

10.1021/jp062311n CCC: $33.50
Published on Web 09/15/2006

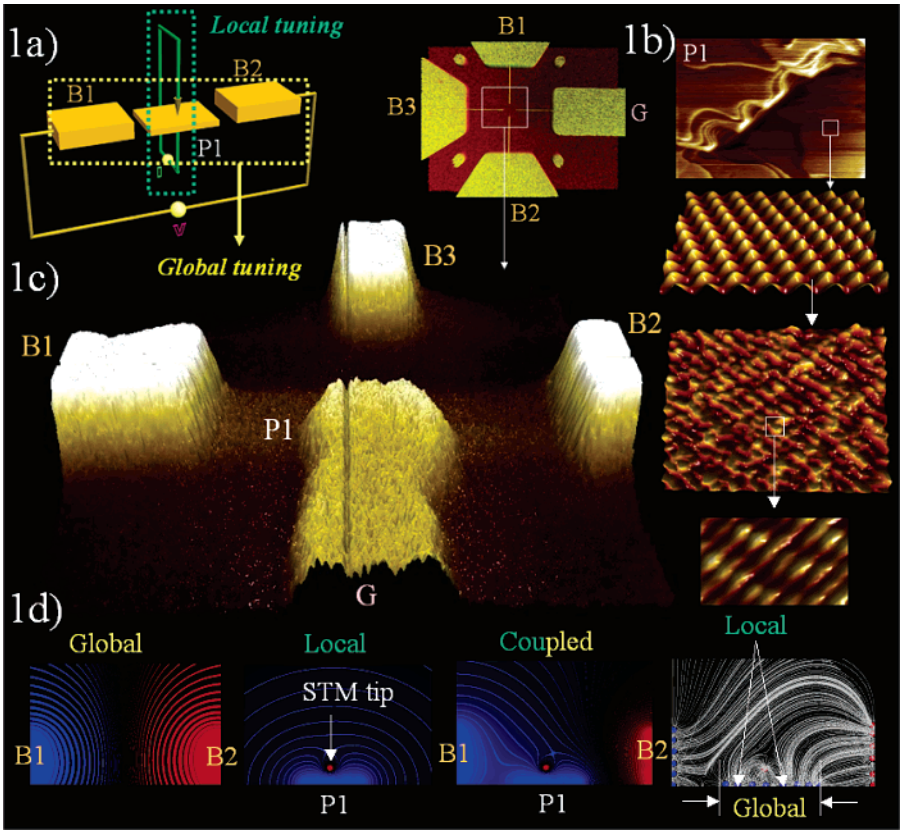

Figure 1. (a) Schematic presentation of experimental setup. B1, B2, and B3 connected to external bias used for global tuning (yellow): P1 is ground and STM tip is connected in series with current voltage (IV) measurement; setup is for local tuning (green). (b) Gold surface on P1 (top), below is a zoomed region Au(111) plane on this gold surface, below is the self-assembled molecular layer of Rose Bengal on this gold substrate, below is the magnified image of molecular layer. (c) AFM image of template wherein it is obvious that B1, B2, and B3 iare at much higher height than P1. (d) Isopotential surface and field gradient for template where there is no P1 and B3, only global force is playing as equivalent of 5 opposite charges of strength 9e; to the right is the same for P1 and vertical STM tip as equivalent of 8e on P1 and 1e on STM tip, hence only local force is playing. To the right is the coupled condition, i.e., both global and local forces are playing. To the extreme right are lines of forces for coupled condition. On P1, only at a particular region, STM−substrate electric field is dominating (local) and surrounding this region is the substrate global bias coupling.

B1−B2−B3) generated electric field so that a conical field generated by a STM tip has a circular projection on P1 around 2−3 nm^2 (both of the same order $\sim 10^7$ V/m, Figure 1). A very high dimensional aspect ratio between global and local interplay allowed this concept to be realized; this is quite clear in isopotential and field gradient plots in pristine local and global cases to the coupled system (Figure 1d).

Second, we have chosen a double planer xanthene dye, Rose Bengal (RB) (Figure 2), which might be permanently twisted for tens of milliseconds into any of 10 possible conformations depending on the trapped position of quasicharge on the molecular backbone. Looking beyond unique "transition dipole" generated rotational dynamics[16] of such systems, we shift from liquid-based in vitro biological experiments to solid-state field-induced torsional dynamics.[17] Rotational jump and momentary cessation of emission (dark state, >10 ms) could be related only by the transition of the whole system into a distinct conformation.[18] Xanthenes undergo complex electron exchange processes in liquid, as quinoid, carboxyl, and hydroxy groups all take part in these processes.[19] But we have considered only single reduction to be present on the molecular backbone and generated 10 possible minimum energy conformations by restricted Hartree−Fock AM1 semiempirical quantum mechanical computation (rms $\sim$ 0.01). Molecular orbital calculations of the ground and excited states have been carried out with Chem3D, CambridgeSoft Corporation, Cambridge, MA, to find the energy minima in the excited state using MOPAC restricted Hartree−Fock (RHF) formalism. To determine exact orientation of a molecular conformation, we followed a well-defined pathway. First, we have identified each conformation by (i) matching the theoretical and experimental STM images, (ii) measuring dimension, height profile, and comparing with theoretical values, (iii) matching dihedral angle between double plane, which changes from 2.72, 88 varying up to −119 among 10 possible conformations. After detection of each state, the very next step was to find exact position of the COOH and OH groups on molecule body to confirm a defined path for current voltage measurement. We identified the COOH position by developing a minimum energy model of each molecular conformation in MAYA 3D animation software and matching the model with the STM image to find the exact location of different functional groups. In more than 80% of cases, we found COOH coupling with the gold surface; others were rejected in further analysis. Then we detected the OH group by voltage variation imaging. We detected definite conformations by comparing total charge density of HOMO with the STM image taken at a positive bias, dihedral angle between planes theoretically and experimentally wherever possible, theoretical and experimental height profile, and finally, current voltage spectrum. AM1 and PM3 computation was used to incorporate various repulsive interactions of RB anion conformations. Repulsive forces dominate when the distance between interacting atoms becomes less than the sum of their contact radii. Repulsion is modeled by an equation that combines an

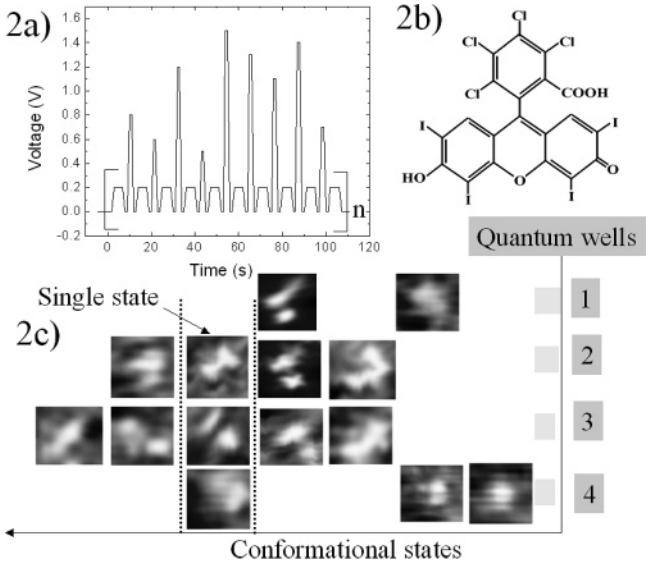

Figure 2. (a) An array of voltage pulses sent to the molecular system between substrate and STM tip for transition to different conformation; between every two pulses, a probe pulse 0.2 V is applied to scan the image. (b) Rose Bengal molecular structure. (c) Successful investigation summary at four quantum wells on P1. In well 1, we see transition between two states only, and in well 3, a random transition between 5 states ias observed. Each conformation appeared differently in different wells before being confirmed by dihedral angle, IV spectrum, and comparing image with theoretical electron density distribution. So on each column a particular conformation sits.

exponential repulsion with an attractive dispersion interaction ($1/R^6$): $E_{\text{vanderWaals}} = \sum_i \sum_j \epsilon(290\,000\, e^{-12.5/R} - 2.25R^{-6})$, where $R = r_{ij}/(R_i^* + R_j^*)$. The parameters include: R_i^* and R_j^* (the van der Waals radii for the atoms), epsilon (ϵ), determines the depth of the attractive potential energy well, and r_{ij} is the actual distance between the atoms. At short distances, the above equation favors repulsive over dispersive interactions. To compensate for this, at short distances ($R = 3.311$), this term is replaced with: $E_{\text{vanderWaals}} = 336.176 \sum_i \sum_j \epsilon R^{-2}$. To include these repulsions and reproduce geometrical variations as observed in STM (Figure 5a,b), we confined our study with AM1 and PM3 even though they do not provide absolute energy values. Also in this particular study, we are interested in difference in energy or transition of states. Inclusion of repulsion also restricts us to study only one monomer because energy minimization with dimer and trimer is not reliable; thus gas-phase values we present here are not the absolute energy required inside the monolayer but provides limiting values of energy required to switch between states.

We begin with the template of Figure 1c fabricated by the combination of e-beam lithography and e-beam evaporation of gold on Si(110) substrate (high resistivity 0.01−0.1 Ω cm), where the horizontal electrode couple (height of B1, B2, and B3 ∼ 100 nm) and processing surface P1 in between (height for P1 ∼ 50 nm) is isolated by ∼80 nm. Increasing electric bias within a certain limit could not induce charge injection to the processing surface P1 as the gap was theoretically simulated, keeping it beyond critical limit. Nanoscale two-stage lithography to generate a height difference of ∼50 nm between the electrode and processing surface decreased the success rate of a final template is around 30%. Processing surface area P1 varied between 100 and 200 nm^2. The large area atomic flat surface of P1 (rms <1.5 nm) and symmetric STM tip (electrochemical etching followed by structure investigation) was essential for global tuning of quantum phenomena. After fabricating a gold template on the Si(110) wafer as above ,we annealed the substrate in a quartz chamber 100% H_2 flow at rate 60 mL/min. This was followed by annealing at temperature 400 °C (600 °C for gold on freshly cleaved mica) with a rise at a rate of 15°/min, stabilized for 30 min, and then sudden switching off the heat source to cool down. The substrate was kept at an optimized angle of 15° in the best operational range of 9−22° with the horizontal axis facing the H_2 gas flow This is very crucial to generate a large area reconstructed atomic flat gold Au(111) substrate. To minimize the defect further, the template is dipped in dimethyl formamide (DMF) solution with continuous tilting of solution with the horizontal axis at a rate of 3°/s for 60 min and no tilting for 2 h. The cycle was repeated 3 times, followed by H_2 annealing as described above. The method described above can generate a large area atomic flat surface (∼500 nm^2 with rms ∼4 nm) with fewer defects than any one method alone. Survival of the final template was around 10%.

The freshly annealed template was soaked in a 1 μM ethanolic solution of RB for 5 h to give rise to 1.2 monolayer coverage self-assembled film (rms ∼ 1.5 nm). Defect states of the monolayer (site without molecule is 2 nm^2, hence we named quantum well) at specific locations were observed at different sections on the surface coverage. Although it was pre-assumed that there were infinite possibilities of conformation (each of 10 states can couple with the environment in several ways hence infinite) in the allowed quantum well unlike the ordered molecular film of Figure 1b, but reality was different (enthalpy ΔH for the interactions that hold molecules together via self-assembly was 12 kcal/nm^2 of a complementary molecular surface[20]). We applied electrical pulse arrays of different height (Figure 2a) and simultaneous STM imaging was carried out in such a way that the scan clock frequency (0.03−20 Hz) and scanning area allowed the STM tip to cross a single molecule area (2 nm^2) within ∼10 ms (the greater the scanning speed and the larger is the area, the faster a molecule is scanned). Continuous transition between different states showed surface−molecular interaction allowed only the few among 10 possible conformational states (Figure 2c) as most probable (reach stable equilibrium) for the confined nanoscale environment or the quantum well. Continuous imaging and identification at a particular site for ∼50 cycles generated Gaussian probabilistic distribution. Philosophically, this result gives us a fundamental truth of nature. Randomness is not as random as it seems; enthalpy (ΔH) never let entropy reach infinity (ΔS), at least in a nanoscale environment; and if not, then they must evolve some constraints to restrict itself in the range of selective choices (here, a few conformational states). The loss in translational entropy in two molecules brought together on gold (111) substrate from solution contributes approximately $-T\Delta S$ (∼6 kcal/mol) to ΔG, where ΔG is Gibbs free energy. Energy release during pulsed transition thus depends on a degree of disorder of the nanoscale environment after transition to different conformations, and minimum change in the internal energy required accommodating with new external energy applied. Individual wells are signified with their range of transitional states on the processing surface.

Results and Discussion

We fabricated both ordered and disordered films on the processing surface P1. Quantum wells in an oriented assembly were more rigid, allowing less conformational transition among polaronic states, as was evident during a continuous pulsed cycle at 40 different sites (>90% of available) on P1 for both kinds of films. In the case of ordered film, conformational transition was extremely selective (1 or 2 states), and in the

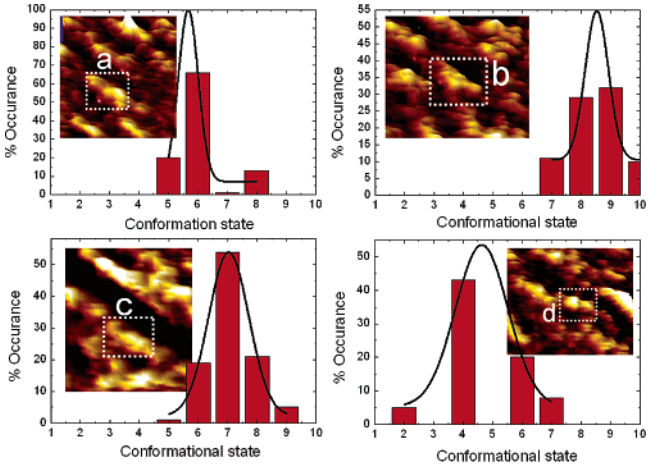

Figure 3. Statistical summery of random transitions in four quantum wells under zero horizontal bias. Inset shows the well under investigation and column shows occurrence for voltage array $n = 9$ and Gaussian fit shows highest Q value for lower stable conformation and remains constant at higher stable conformations. Energy for states 1, 2, 3, 4, 5, 6, 7, 8, 9, and 10 are as follows: −61, −80, −83, −85.5, −89, −91, −96.92, −97.7, −97.95, and −104.54 kcal, respectively. In well a, the surrounding environment allows energy around −90 kcal and provides highest stability. If the local environment plays a major role, then energetically lower stable states might become most favorable as in well d. Hence well b has the least environment effect and well c has midway between a and b.

case of disordered film, conformational transition varied between 3 or 4 states, but a periodic pulsed cycle did not generate conformational states periodically in the same order. However, we could gather information for ∼50 cycles, a maximum at a typical well (30 sites total) before molecules could fatigue under random pulse, and plotted the probability of finding each state during this transition (statistical database of 1500 cases). If we consider the lowest minimum energy conformation as state 10 (−104.54 kcal) and highest as state 1 (−61 kcal), then the probability distribution shows as a Gaussian distribution (Figure 3a,b,c,d) over the energy range.

The quality factor (Q value)[21] reveals the bandwidth of allowed energy exchange in a well. In the quantum well, the variation of energy barrier should exchange energy discretely varying between ∼0.2 and 40 kcal for transition to different states. Transitional energy includes the energy fluctuation via dimerization ($\Delta E \sim -10$ kcal),[22] as was evident in current enhancement beyond the molecular boundary in the current spectrum of continuous image tunneling spectroscopy (CITS) response both in the fuzzy and oriented assembly. The molecular dynamics simulated a self-assembled structure of 10 molecules (single RB $\sim 1.6 \times 1.5$ nm^2) on a $25 \times 25 \times 4$ Au(111) atomic matrix showed vertical positioning of the lower plane in arrays supporting the STM image of Figure 1. For such orientation of molecules, change in EDD for HOMO (positive bias) and LUMO (negative bias) is not differentiable by the shape of orbital density ($|\sum \Psi_i(r)|^2$). As vertical bias increased, cross-sectional enhancement of higher current mapping could be due to an increment in interaction between horizontal chlorine-dominated planes (at V1 and V4 of Figure 4a).

Such a sudden signal enhancement between molecules even in a vibronic spectrum could be due to vibronic band−MO coupling.[23,24] This kind of instability might be due to potential energy generated from a dipole−dipole interaction, which destabilized the surface−molecule interaction.[25] Spatial distribution of the local field on a substrate just below the tip dies out rapidly beyond critical radius if we move radially outward from

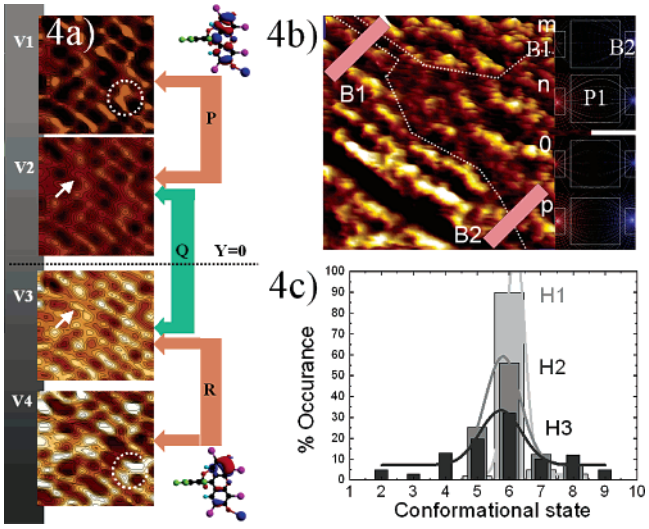

Figure 4. (a) CITS image at V1, V2, V3, and V4: −0.8, −0.3, 0.3, and 0.8 V, respectively, on ordered film of Rose Bengal. Circular dotted region in V1 and V4 shows enhanced interaction between chlorine-dominated planes, arrow in V2 and V3 shows significant current transition between LUMO and HOMO probe, $Y = 0$ denotes the Fermi level of the system. Top and bottom molecular image of Rose Bengal shows LUMO and HOMO orbitals, respectively. (b) Disordered film of RB and B1 and B2 are electrode directions, m, n, o, p are the horizontal bias generated electric field and potential gradients; B1 is positive 9e (red), and B2 is negative −9e (blue). (c) Control of molecular at H1 = 6 V, H2 = 0 V, H3 = 12 V (see tuning in supporting movie online).

center.[6] The effect of horizontal bias inside this very local region is limited, although it makes the local boundary even sharper. Interestingly, (Figure 4b) once horizontal bias is applied, the system already reached equilibrium with the external field and degree of perturbation by the STM tip could not completely erase the global signature. This signature depends on (i) stabilization of molecule at different conformations, (ii) local and global bias, and (iii) the flexibility of the electrode system generating random isopotential coupling on P1 (looking beyond more than three electrodes). We took the current voltage property of these polarons of RB (shown in Figure 5a,b) and found that in some cases they are ohomic and in some cases they are insulating or semiconducting or providing constant current output for certain ranges. This focuses a light on debates of the true mechanism for bistable switching.[22]

In a particular well occupying molecule, we varied both horizontal (B1−B2 case) and vertical bias by following the schematic of Figure 1a and identifying the transition of molecular conformation. Over the processing surface P1 (Figure 1), there is stochastic distribution of available conformation bands (containing 2 or 3 states among 10) for spatial distribution of wells. Gaussian probabilistic distributions generated in each well were plotted for different horizontal bias conditions. If horizontal bias is increased in a loop $(-V_{min} \rightarrow +V_{max} \rightarrow -V_{min} \rightarrow +V_{max})_n$, keeping vertical bias constant, in a particular well, the Q value of the distribution could be changed significantly (Figure 4c); at 6 V, we could confine states less than 25%, while at 12 V, noise destroys control. Variation of Q values at different locations is different; an example is given in the Supporting Information movie.

Conformational transition studies were performed with fluorescein sodium and eosin Y, two other molecules with fewer acceptor groups and a single planar quinone derivative DDQ. We found that the more the number of electroactive sites and structural flexibility of a molecule, the greater the possibility

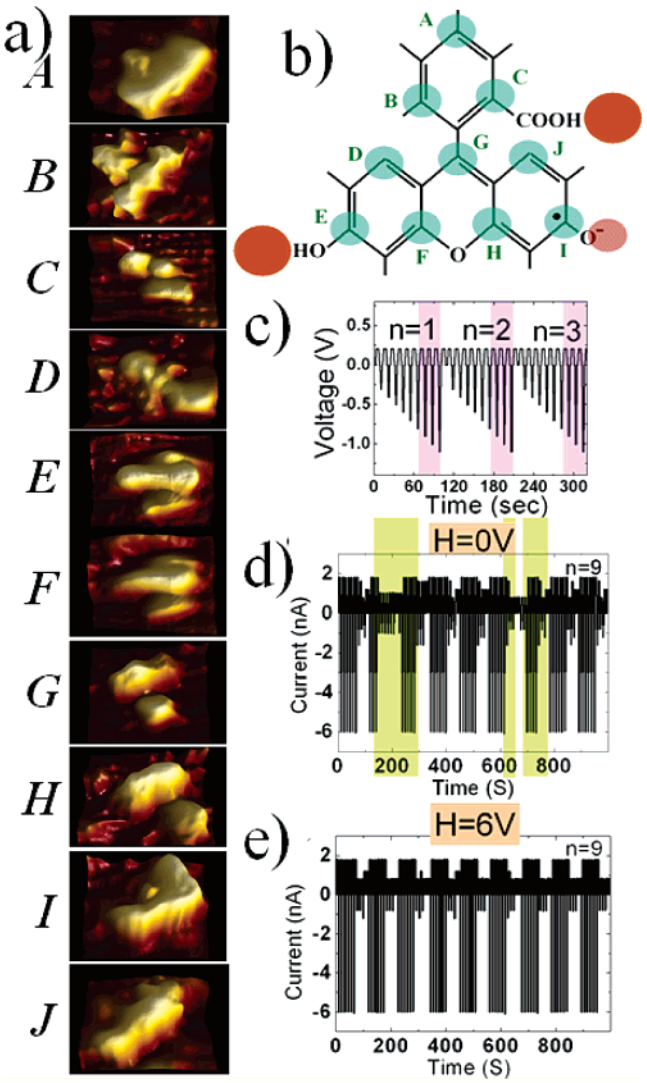

Figure 5. (a) STM images of the 10 most common conformations of singly reduced Rose Bengal molecules in a disordered film, all images are 1.5 × 2 nm^2, height 0.6 nm. Minimum energy conformation and dimension of each conformation were A = −97.95 kcal (1.6 × 0.9 × 0.5 nm^3), B = −85.5 kcal (1.5 × 1 × 0.51 nm^3), C = −97.7 kcal (1.6 × 1.5 × 0.48 nm^3), D = −61 kcal (1.6 × 1.4 × 0.5 nm^3), E = −89 kcal (1.6 × 1.3 × 0.5 nm^3), F = −83 kcal (1.6 × 0.6 × 0.5 nm^3), G = −96.92 kcal (1.4 × 1.2 × 0.52 nm^3), H = −80 kcal (1.5 × 1.5 × 0.5 nm^3), I = −104.54 kcal (1.5 × 0.9 × 0.51 nm^3), J = −91 kcal (1.6 × 1.2 × 0.52 nm^3). 1 kcal/moL = 0.043 eV where kT = 0.023 eV in 300 K. (b) The electron trap sites on the molecule corresponding to the 10 conformations A−J, according to modeling. Black dot illustrates trapped electron at site I. (c) Array of voltage pulses (width 2 s, imaged at positive bias 0.2 V) applied to molecules in disordered film; regions where critical voltage is exceeded (see text) are shown by shading. (c) Experimentally measured current induced by voltage array (panel b) without horizontal field; shading indicates dead regions (see text). (e) Same as (d), but with horizontal field of 6 V; note absence of dead regions.

that it stabilizes into many minimum energy conformations generating a "dead zone" and even getting into a "permanent twist". The similar results were also obtained by T. Ha et al., where they found that the equilibrium population of rapidly rotating states varied from zero for CY5 to 100% for tetramethylrodamine. The molecular system could be extended further for realization of multilevel conductivity[26] and multilevel switches ($S = \{\Omega_i\}$, $\Omega_{max}/\Omega_{min} = 330$ at 1.02 V), biospecies interactions[27] such as RB is well-known for its similar performances and monomolecular electronics with molecular-state control in a self-assembled matrix.[28]

High field gradient generation for nanoscience is not new. Global fields have been applied to develop several devices.[6c,29] But the physical situation is unique in our case because of multiple parameter control, a claim which needs a further experiment and review of the results obtained in Figure 4c. The evidence of this proposition is shown in Figure 5c,d,e in a very similar experiment of Figure 4c; instead of probability of states, we have plotted the current output directly.

Here we select state D of RB, which provides constant current output of −6 nA and 2 nA if the bias applied is less than ±0.8 V. If the state (D) is changed into any other (A → J) states, current will fall obviously as other states do not have this feature as mentioned earlier. We fix the STM tip on this species after identification, switch off feedback loop, and apply the pulsed array of Figure 5c. We observe that when there is no horizontal bias several times, the species is converted into another species suddenly and comes back spontaneously (Figure 5d).[14] As a result, we observe conductivities corresponding to other species even though the pulse is less than 0.8 V (less probe current is expected because only one species can show such performances, hence we call this a dead region). But when we apply horizontal bias, then we observe that the species under study does not change suddenly into another state and it performs continuously (Figure 5e). Apart from providing further evidence of our dual mode control as observed in Figure 4c, it also emphasizes the existence of some other local parameter that exchanges charge via direct or superexchange[31,32] or makes local conformational changes. Thus we can say in general that, on P1, each molecule trapped in a quantum well is modified by four potentials generated by horizontal bias (V_Z), vertical bias (V_P), conformational fluctuation of neighboring molecules by horizontal bias (V_{eff}),[30] and coordination sphere fluctuation via electron transfer by global and local bias ($V_{polaron}$).[6] Current through the molecule is function of four potentials $I = f(V) = f(V_Z, V_P, V_{eff}, V_{polaron})$. Vertical projection of field distribution on the substrate surface showed a centrally uniform field immediately below the STM tip's face and falls off at distances greater than the radius of the tip facet. Geometrical field enhancement is very local on the substrate surface, and the surrounding environment could perturb the local system. Stabilization by global bias is basically tuning preferable conformational change with an average field V_{eff}. Here, the tip-generated local field ∼10^7 V/m (e.g., 0.05 V/2nm) and the surrounded electrode-generated global electric field of the order ∼10^7 V/m (e.g., 5 V/300 nm) interplay with each other and we could generate different architecture and field order for case-selective studies of our choice.

Conclusion

In conclusion, dual mode tuning has revealed that conformation and electronic transitions are not a separate issue for molecular systems, hence the original mechanism of electronic property generated might be an interplay of both. As our tool is smart enough to isolate electronically and mechanically a system even within ∼2 nm^2 area and restrict its spontaneous conformational transition within only a few possible choices, we can directly view the action of individual molecules without need to infer analyzing processes from its static form. Although the control we have achieved is statistical and not a well-defined single molecule state into a very well predicted final state, we have presented an alternative way that is sure to be improved in the near future with the inclusion of more surrounding electrodes around P1. With more variable global field control,

the presented technique of dual mode tuning might provide much better understanding of how a phenomenon is generated in a nanoscale and finally evolve as global properties in many natural systems around us.

Acknowledgment. This study is performed through the special coordination fund from the Ministry of Education, Culture, Sports, Science, and Technology (MEXT) of the Japanese Govt.

Supporting Information Available: Two movie files captured in 1.5×1.6 nm^2 area during dual mode operation at H2 = 0 V and at H4 = 8 V, showing control by dual mode is provided. This material is available free of charge via the Internet at http://pubs.acs.org.

References and Notes

(1) (a) Donhauser, Z. J.; Mantooth, B. A.; Kelly, K. F.; Bumm, L. A.; Monnell, J. D.; Stapleton, J. J.; Price, D. W., Jr.; Rawlett, A. M.; Allara, D. L.; Tour, J. M.; Weiss, P. S. *Science* **2001**, *292*, 2303. (b) Emberly, E. G.; Kirczenow, G. *Phys. Rev. B* **2001**, *64*, 235412.

(2) (a) Chang, L.; Choi, Y.; Ha, D.; Ranade, P.; Xiong, S.; Bokor, J.; Hu, C.; King, T. *Proc. IEEE* **2003**, *91*, 1860. (b) Zhirnov, V. V.; Cavin, R. K.; Hutchby, J. A.; Bourianoff, G. I. *Proc. IEEE* **2003**, *91*, 1934.

(3) (a) Thielmann, A.; Hettler, M. H.; König, J.; Schön, G. *Phys. Rev. B* **2003**, *68*, 115105. (b) Selzer, Y.; Cai, L.; Cabassi, M. A.; Yao, Y.; Tour, J. M.; Mayer, T. S.; Allara, D. L. *Nano Lett.* **2005**, *5*, 61. (c) Seminario, J. M.; Cruz, C. E. D. L.; Derosa, P. A. *J. Am. Chem. Soc.* **2001**, *123*, 5616. (d) Butts, M.; DeHon, A.; Goldstein, S. C. *Proceedings of the 2002 IEEE/ACM International Conference on Computer-Aided Design, 2002, San Jose, CA, November 10−14, 2002*; IEEE/ACM: New York, 2002; p 433.

(4) (a) Kornilovitch, P. E.; Bratkovsky, A. M. *Phys. Rev. B* **2001**, *64*, 195413. (b) Emberly, E. G.; Kirczenow, G. *Phys. Rev. Lett.* **2003**, *91*, 188301. (c) Bratkovsky, A. M.; Kornilovich, P. E. *Phys. Rev. B* **2003**, *67*, 115307.

(5) Datta, S. *Electronic Transport in Mesoscopic Systems*; Cambridge University Press: New York, 1995; p-293.

(6) (a) Campbell, P. A.; Fernan, G. A.; Walmsley, D. G. *Nanotechnology* **2002**, *13*, 69. (b) Rabitz, H.; Vivie-Riedle, R.; Motzkus, M.; Kompa, K. *Science* **2000**, *288*, 824. (c) Schultz, S. A.; Bethlem, H. L.; Veldhoven, J. D.; Küpper, J.; Conrad, H.; Meijer, G. *Phys. Rev. Lett.* **2004**, *93*, 020406.

(7) (a) Sasahara, A.; Uetsuka, H.; Onishi, H. *Phys. Rev. B* **2001**, *64*, 121406. (b) Taylor, J.; Brandbyge, M.; Stokbro, K. *Phys. Rev. B* **2003**, *68*, 121101. (c) Cahen, D.; Kahn, A.; Umbach, E. *Mater. Today* **2005**, *August*, 32. (d) Tsiper, E. V.; Soos, Z. G. *Phys. Rev. B* **2003**, *68*, 085301. (e) Tsiper, E. V.; Gao, W.; Soos, Z. G.; Kahn, A. *Chem. Phys. Lett.* **2002**, *360*, 47. (f) Amy, F.; Chan, C.; Kahn, A. *Org. Electrochem.* **2005**, *6*, 85.

(8) (a) Langowski, S.; Wachmuth, M.; Waldeck, W. *Biophys. J.* **2000**, *78*, 2272. (b) Service, R. F. *Science*, **1999**, *283*, 1668. (c) Mehta, A. D.; Reif, M.; Spudich, J. A.; Smith, D. A.; Simmons, R. M. *Science* **1999**, *283*, 1689. (c) http://ourworld.compuserve.com/Homepages/KatrinKneipp/SMDatMIT.htm.

(9) (a) Hu, Y.; Zhu, Y.; Gao, H.; Guo, H. *Phys. Rev. Lett.* **2005**, *95*, 156803. (b) Neuman, D. A. *Mater. Today* **2006**, *9*, 34. (c) Fischer, P.; Kim, D.-H.; Chao, W.; Liddle, J. A.; Anderson, E. H.; Attwood, D. T. *Mater. Today* **2006**, *9*, 26.

(10) (a) Dickson, R. M.; Cubitt, A. B.; Tsien, R. Y.; Moerner, W. E. *Nature* **1997**, *388*, 355. (b) Dougherty, W. M.; Bruland, K. J.; Garbini, J. L.; Leath, W. M.; Sidles, J. A. *Cell Vision* **1997** *4*, 134. (c) Brouwer, A. C. J.; Groenen, E. J. J.; Schmidt, J. *Phys. Rev. Lett.* **1998**, *80*, 3944.

(11) (a) Kataoka, N.; Saito, K.; Sawada, Y. *Phys. Rev. Lett.* **1999**, *82*, 1075. (b) Drexler, K. E. *Engines of Creation*; Anchor Books: New York, 1986; http://www.foresight.org/EOC/.

(12) (a) Chaudhuri, D.; Chang, S.; Demaria, C. D.; Alvania, R. S.; Soong, T. W.; Yue, D. T. *J. Neurosci.* **2004**, *24*, 6334. (b) Cavalcanti, A.; Freitas, R. A., Jr.; Kretly, L. C.; *DETC2004, ASME Design Engineering Technical Conferences, 28th Biennial Mechanisms and Robotics Conference, Salt Lake City, Utah*, 2004; pp 1−10. (c) Brown, R.; Gallop, J.; Milton, M. *Review of Techniques for Single Molecule Detection in Biological Applications*; NPL Report COAM2; National Physical Laboratory: Teddington, Middlesex, U.K., 2001; p 38.

(13) (a) DiStefano, J. J., III.; *Ann. Biomed. Eng.* **1976**, *4*, 302. (b) DiStefano, J. J., III.; *J. Cybernetics Inf. Sci.* **1979**, *2*, 6. (c) Dekker, C.; Ratner, M. A. *Phys. World* **2001**, 14, 29. (d) Porath, D.; Bezryadin, A.; De Vries, S.; Dekker, C. *Nature* **2000**, *403*, 635.

(14) (a) Hettler, M. H.; Wenzel, W.; Wegewijs, M. R.; Schoeller, H. *Phys. Rev. Lett.* **2003**, *90*, 076805. (b) Nirmal, M.; Dabbousi, B. O.; Bawendi, M. G.; Macklin, J. J.; Trautman, J. K.; Harris, T. D.; Brus, L. E. *Nature* **1996**, *383*, 802. (c) Ha, T.; Enderle, T.; Chemla, D. S.; Selvin, P. R.; Weiss, S. *Chem. Phys. Lett.* **1997**, *271*, 1.

(15) (a) Nishiyama, Y.; Allakhverdiev, S. I.; Yamamoto, H.; Hayashi, H.; Murata, N. *Biochemistry* **2004**, *43*, 11321. (b) Campagnola, P. J.; Delguidice, D. M.; Epling, G. A.; Hoffacker, K. D.; Howell, A. R.; Pitts, J. D.; Goodman, S. L. *Macromolecules* **2000**, *33*, 1511. (c) Stevelmans, S.; van Hest, J. C. M.; Jansen, J. F. G. A.; van Boxtel, D. A. F. J.; de Brabander-van den Berg, E. M. M.; Meijer, E. W. *J. Am. Chem. Soc.* **1996**, *118*, 7398. (d) Carreon, J. R.; Roberts, M. A.; Wittenhagen, L. M.; Kelley, S. O. *Org. Lett.* **2005**, *7*, 99. (e) Miklis, P.; Cagin, T.; Goddard, W. A., III. *J. Am. Chem. Soc.* **1997**, *119*, 7458.

(16) (a) Ha, T.; Enderle, Th.; Chemla, D. S. *Phys. Rev. Lett.* **1996** *77*, 3979. (b) Sase, I.; Miyata, H.; Ishiwata, S.; Kinosita, K., Jr. *Proc. Natl. Acad. Sci. U.S.A.* **1997**, *94*, 5646.

(17) (a) Vamosi, G.; Gohlke, C.; Clegg, R. M. *Biophys. J.* **1996**, *71*, 972. (b) Fourkas, J. T. *Opt. Lett.* **2001**, *26*, 211. (c) Lieb, M. A.; Zavislan, J.; Novotny, L. *J. Opt. Soc. Am. B* **2004**, *21*, 1210 and references therein.

(18) (a) Ha, T.; Glass, J.; Enderle, T.; Chemla, D. S.; Weiss, S. *Phys. Rev. Lett.* **1998**, *80*, 2093. (b) Mei, E.; Vinogradov, S.; Hochstrasser, R. M. *J. Am. Chem. Soc.* **2005**, *125*, 2730. (c) Deschenes, L. A.; Vanden Bout, D. A.; *Science* **2001** *292*, 255. (d) Bartko, A. P.; Xu, K. W.; Dickson, R. M. *Phys. Rev. Lett.* **2002**, *89*, 026101.

(19) Margulies, D.; Melman, G.; Shanzer, A. *Nat. Mater.* **2005**, *4*, 768.

(20) Sharp, K. A.; Nicholls, A.; Fine, R. F.; Honing, B. *Science* **1991** *252*, 106.

(21) In a fitted gaussian distribution pattern Occurance(state) = $[(1/\sqrt{2\pi\sigma^2})\ e^{-(\text{state}-a)^2/2\sigma^2}]$ where a is the mean and σ is the standard deviation. We select two points on the graph, one at −1/e of the peak value and one at +1/e value of the peak value. Then the state width at Δ1/e, i.e., state axis projected value (Val(1/e) − Val(−1/e)) is called Q value.

(22) Bandyopadhyay, A.; Pal, A. J. *J. Phys. Chem. B* **2005**, *109*, 6084.

(23) Hipps, K. W.; Hoagland, J. J. *Langmuir* **1991**, *7*, 2180.

(24) Pascual, J. I.; Gómez-Herrero, J.; Sánchez-Portal, D.; Rust, H.-P. *J. Chem. Phys.* **2002**, *117*, 9531.

(25) (a) Nguyen, Q. T.; Glinel, K.; Pontié, M.; Ping, Z. *J. Membr. Sci.* **2004**, *232*, 123. (b) http://www.nist.gov/sigmaxi/Posters00/Abst/Saupe-abs.html. (c) Petrovykh, D. Y.; Pérez-Dieste, V.; Opdahl, A.; Kimura-Suda, H.; Sullivan, J. M.; Tarlov, M. J.; Himpsel, F. J.; Whitman, L. J. *J. Am. Chem. Soc.* **2006**, *128*, 2. (d) Hovis, J. S.; Liu, H.; Hamers, R. J. *Appl. Phys. A* **1998**, *66*, S553.

(26) (a) Li, Q.; Mathur, G.; Homsi, M.; Surthi, S.; Misra, V.; Malinavskii, V.; Schweikart, K.; Yu, L.; Lindsey, J. S.; Liu, Z.; Dabke, R.; Yasseri, A.; Bocian, D.; Kuhr, W. *Appl. Phys. Lett.* **2002**, *81*, 1494. (c) Roth, K. M.; Dontha, N.; Dabke, R.; Gryko, D.; Clausen, C.; Lindsey, J.; Bocian, D.; Kuhr, W. *J. Vac. Sci. Technol., B* **2000**, *18*, 2359. (d) Rozenberg, M. J.; Inoue, I. H.; Sánchez, M. J. *Phys. Rev. Lett.* **2004**, *92*, 178302. (e) Li, C.; Fan, W.; Lei, B.; Zhang, D.; Han, S.; Tang, T.; Liu, X.; Liu, Z.; Asano, S.; Meyyappan, M.; Han, J.; Zhow, C. *Appl. Phys. Lett.* **2004**, *84*, 1949. (f) Bandyopadhyay, A.; Pal, A. J. *Appl. Phys. Lett.* **2004**, *84*, 999.

(27) (a) http://www.almaden.ibm.com/st/projects/nanoscale/mrfm/. (b) Wooley, A. T.; Cheung, C. L.; Hafner, J. H.; Lieber, C. M. *Chem. Biol.* **2000**, *7*, R193. (c) Arakawa, H.; Umemura, K.; Ikai, A. *Nature* **1992**, *358*, 171.

(28) (a) Stadler, R.; Ami, S.; Forshaw, M.; Joachim, C. *Nanotechnology* **2003**, *14*, 722. (b) Ellenbogen, J. C.; Love, J. C. *Proc. IEEE* **2000**; 88, 386.

(29) (a) Kerman, A. J.; Sage, J. M.; Sainis, S.; Bergeman, T.; DeMille. D. *Phys. Rev. Lett.* **2004**, *92*, 033004. (b) DeMille, D. *Phys. Rev. Lett.* **2002**, *88*, 067901.

(30) (a) Feynman, R. P.; Hibbs, A. R. In *Quantum Mechanics and Path Integrals*; McGraw-Hill: New York, 1965. (b) Callaway, D.; Rahman, A. *Phys. Rev. Lett.* **1982**, *49*, 613. (c) Nicholas, A. L.; Shandler, D.; Singh, V.; Richardson, D. M. *J. Chem. Phys.* **1984**, *81*, 5109. (d) Scharf, D.; Landman, U.; Jortner, J. *J. Chem. Phys.* **1987**, *87*, 2716. (e) Ramirez, R.; Schulte, J.; Bohm, M. C. *Chem. Phys. Lett.* **2005**, *402*, 346. (f) Benedek, G.; Martin, T. P.; Pacchioni, G. Elemental and Molecular Clusters. In *Proceedings of the 13th International School, Erice, Italy, 1987; Molecular Clusters*; Jortner, J., Scharf, D., Landman. U., Eds.; Springer-Verlag: New York; 1987; p 148.

(31) Rust, M.; Lappe, J.; Cave, R. J. *J. Phys. Chem. A* **2002**, *106*, 3930.

(32) Hochhauser, I. L.; Taube, H. *J. Am. Chem. Soc.* **1947**, *69*, 1582.